

Lab on a Chip

Accepted Manuscript



This is an *Accepted Manuscript*, which has been through the Royal Society of Chemistry peer review process and has been accepted for publication.

Accepted Manuscripts are published online shortly after acceptance, before technical editing, formatting and proof reading. Using this free service, authors can make their results available to the community, in citable form, before we publish the edited article. We will replace this *Accepted Manuscript* with the edited and formatted *Advance Article* as soon as it is available.

You can find more information about *Accepted Manuscripts* in the [Information for Authors](#).

Please note that technical editing may introduce minor changes to the text and/or graphics, which may alter content. The journal's standard [Terms & Conditions](#) and the [Ethical guidelines](#) still apply. In no event shall the Royal Society of Chemistry be held responsible for any errors or omissions in this *Accepted Manuscript* or any consequences arising from the use of any information it contains.

TECHNICAL INNOVATION

Non-equilibrium electrokinetic micromixer with 3D nanochannel networks†

Cite this: DOI: 10.1039/x0xx00000x

Eunpyo Choi, Kilsung Kwon, Seung Jun Lee, Daejoong Kim* and Jungyul Park*

Received 00th January 2012,
Accepted 00th January 2012

DOI: 10.1039/x0xx00000x

www.rsc.org/

We report an active micromixer which utilizes vortex generation due to non-equilibrium electrokinetics near the interface between microchannel and nanochannel networks membrane (NCNM) constructed by geometrically controlled *in situ* self-assembled nanoparticles. The large interfacing area where possible vortices are generated can be realized, because nano-interstices between these assembled nanoparticles are intrinsically the collective three-dimensional nanochannel networks compared to the typical silicon based 2D nanochannels. The proposed mixer shows 2-folds shorter mixing time (~0.78 ms) and 34-folds shorter mixing length (~7.86 μm) as compared to conventional 2D nanochannels, in direct.

Introduction

The advanced micro/nano fluidic system integrated with the assembled micro/nanostructures in microchannels can be utilized for various issues in micro-total analysis systems (μ -TAS).¹⁻⁸ For example, Choi *et al.* proposed the chemical gradients generator for bacterial chemotaxis study using the micro-sized channel networks from the self-assembly of micro-sized particles.¹ The stable and robust chemical gradient could be realized by allowing the transport of both ions and molecules through the micro-interstices which formed in the closed-packed microparticles. A disposable rapid on-chip using the hetero-packed beads at the inlet of a microchannel was proposed as a microfilter system for whole blood/plasma separation.²

The assembled nanoparticles can also be adopted for diverse range of applications by inducing electrokinetic phenomena in microfluidics.³⁻⁸ The microplatform based on reverse electrodialysis was presented, which enables high ionic flux through three dimensional nanochannel networks for high power energy generation.³ These three dimensional nanochannel networks that have a role of effective cation-selective membrane are created between two microfluidic channels using geometrically controlled *in situ* self-assembled nanoparticles. Zeng *et al.* suggested the biomolecule sieving system based on the use of ordered colloidal arrays to define the sieve structure within a microfluidic device.⁴ Under the moderate electric fields, they achieved the fast separation of DNA and proteins of a wide size range. Lei *et al.* reported an approach utilizing a suspended nanoparticle crystal as an electrical read-out biosensor based on a nanofluidic electrokinetics principle.⁵ Especially, an imbalance of electrolyte concentrations nearby perm-selective membrane under DC bias, called an ion concentration polarization (ICP),⁹ occurs due to overlapping of electrical double layers in the assembled nanoparticles.⁶⁻⁸ ICP has great potential for engineering applications such as chemical mixing,¹⁰ biomolecule concentration,¹¹ and water desalination,¹² *etc.*, because it is capable of controlling, on demand, any charged species in the electrolyte.⁹ ICP phenomena around the assembled nanoparticles can be visualized in the PDMS channel and characterized its electrokinetics

by varying the geometries of microchannel and materials and size of the nanoparticles.⁶ Furthermore, the water desalination was demonstrated by using this ICP phenomena near the assembled nanoparticles⁷ and Syed *et al.* suggested the electrokinetic preconcentration system based on ICP near the nanoparticle assembly which allowed rapid concentration of DNA and the protein samples.⁸

In this paper, we present the active micromixer which utilizes vortex generation due to non-equilibrium electrokinetics near the interface between microchannel and the assembled nanoparticles (**Fig. 1(a)**). Previously, Kim *et al.* proposed the practical micromixer design which allows efficient vortex generation due to non-equilibrium electrokinetics near the silicon based straight nanochannels.¹³ It was improved using multiple-arraying the nanochannel as shown in **Fig. 1(b)**, and the mixing time was quantified in different operating conditions, *e.g.*, concentration, electric fields, and flow rate.¹⁰ However, since the array of nanochannels were realized in two dimensions (2D) through a top-down e-beam based fabrication, it is fundamentally difficult to increase the confined interfacing area (possible area to induce the vortex). Also it requires heavy fabrication process and equipment. The proposed system can have higher mixing performance by using the self-assembled nanoparticles, which allows the large effective interfacing area. It is because the nano-interstices between the assembled nanoparticles function as the collective three-dimensional (3D) nanochannel networks, compared to conventional silicon based nanochannel corresponding to a thin one-dimensional pathway. Therefore, the shorter mixing time and shorter mixing length can be attained in the proposed system. The mixing performance is characterized by changing the nanoparticle size and is also compared with the aforementioned straight nanochannel method.^{10, 13} We finally obtained about 2-folds shorter mixing time and 34-folds shorter mixing length in average by using the optimally selected nanoparticles.

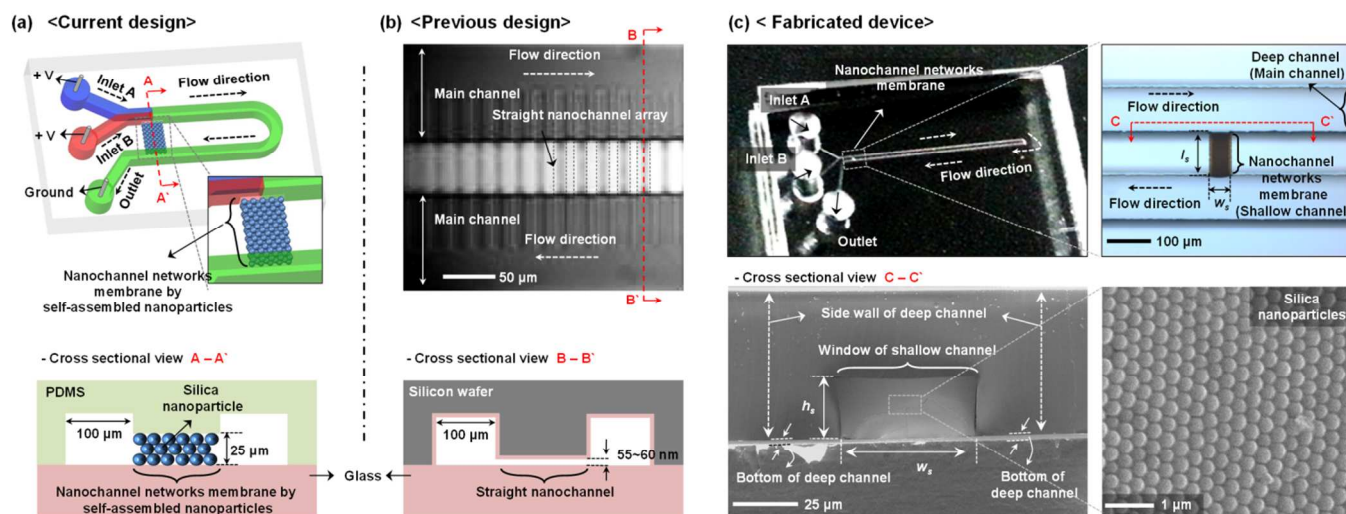


Fig. 1 (a) Schematic illustration of proposed micromixer device. (b) Conventional design of micromixer device. Insert microscope image is taken from Lee *et al.*¹⁰ (c) Upper picture shows the fabricated micromixer device (left) and its enlarged microscopic images (right). Lower picture shows SEM images of the fabricated device at cross-section in the direction of C-C' (left) and its enlarged image at the middle of the window of shallow channel (right).

Results and discussions

Sec. I and II in ESI† shows the formation of the nanochannel networks using nanoparticles within the shallow channel, as reported previously^{1, 3, 6}. The spatially controlled self-assembly of nanoparticles within the microchannel was realized by the multi-layered design of microchannels and controlling the microdroplet containing nanoparticles. **Fig. 1(c)** shows fully filled with the self-assembled nanoparticles in a face centered cubic (FCC) structures within the shallow channel. The nano-interstices formed in these closed-packed nanoparticles of homogeneous sizes, which consist of equivalent nanopores (~15 % of the sphere size),⁴ serve as the pores of ion-selective membranes at a low ionic strength, because the so-called Debye layer thickness (λ_D : 30.7 nm at 0.1 mM KCl) is comparable with the size of the nanopores in these nano-interstices (when D_n is 240 nm, 300 nm, and 700 nm, nanopore size is 36, 45, and 105 nm, respectively).¹⁴ Previously, Choi *et al.* used these nanopore clusters as ion-selective membranes, which are stacked in 3D with interconnection with one another, and called this as “nanochannel networks membrane (NCNM)”⁶.

When a DC voltage is applied, ion concentration polarization (ICP) occurs near NCNM as follows.^{6, 15} At the anodic side, positive ions can transport into the perm-selective NCNM but negative ions are expelled from the NCNM. The condition of overall electro-neutrality forces the concentrations of both cations and anions to decrease in the anodic side of NCNM and induce concentration gradients. Because of these concentration gradients, a preferential cation transport through NCNM is satisfied across the entire system while maintaining a net zero anion flux. The ion transport and concentration are limited in the boundary region (diffusion layer) near NCNM. A further increased electric field results in the breakup of the ICP structure, generating vortices near NCNM.^{10, 16} The strong vortices are the result of electrokinetics at its non-equilibrium state which mix the two fluid streams as shown in **supplementary movie, ESI†**. We used potassium chloride (KCl) solutions with 0.1 mM concentration for all experiment at which previous study by Lee *et al.*¹⁰ had obtained best mixing performance. The voltage from a source meter was applied through platinum electrodes. For visualization purpose, we mixed one stream with fluorescent dye.

Fig. 2(a) shows the fluorescent image and its normalized intensity profiles in y direction from upstream (red line), near the NCNM (blue line) and downstream (green line). Here, we used the silica nanoparticles of 300 nm diameters and flow rate of 3 $\mu\text{L}/\text{min}$. When the voltage of 200 V is applied, the strong vortex structure is observed near the NCNM. Therefore, the two laminar flows from upstream become mixed apparently near the NCNM and the mixing is complete at the downstream. Based on these results, we compare the mixing performance by varying the diameters of the nanoparticles (D_n). We used the normalized mixing index, I_{norm} , obtained from fluorescent intensity data to quantify mixing. It can be defined as follows.^{10, 13}

$$I_{norm}(x) = \left(1 - \frac{\int_{y_{min}}^{y_{max}} |I(y) - I_{100\%}| dy}{\int_{y_{min}}^{y_{max}} |I_{0\%} - I_{100\%}| dy} \right) \quad (1)$$

here, $y_{min} = -42 \mu\text{m}$, $y_{max} = 42 \mu\text{m}$. The fluorescent intensity, $I(y)$, was probed across the width of a deep channel in y direction. From $I(y)$, we calculate a normalized mixing index, $I_{norm}(x)$. The coordinate x starts from the point where the flow first meets NCNM (x - y coordinates are depicted more details in **Fig. 2(a)**). $I_{100\%}$ and $I_{0\%}$ indicate a fluorescent intensity for perfect mixing and non-mixing, respectively. **Fig 2 (b) to (d)** show the profiles of normalized mixing index along the fluid flow for the variation in applied voltages at 700 nm, 300 nm, and 240 nm of D_n , respectively. We changed applied voltages between 100 V and 200 V with the other experimental conditions fixed at 3 $\mu\text{L}/\text{min}$ of flow rate. The overall trends show that the mixing completion ($I_{norm} \sim 1$) occurs further upstream with the increased applied voltage. This result is in reasonable agreement with the previous work by Kim *et al.*^{10, 13} The higher applied voltage promotes the stronger non-equilibrium electrokinetic phenomena near NCNM and thereby improves mixing performance.

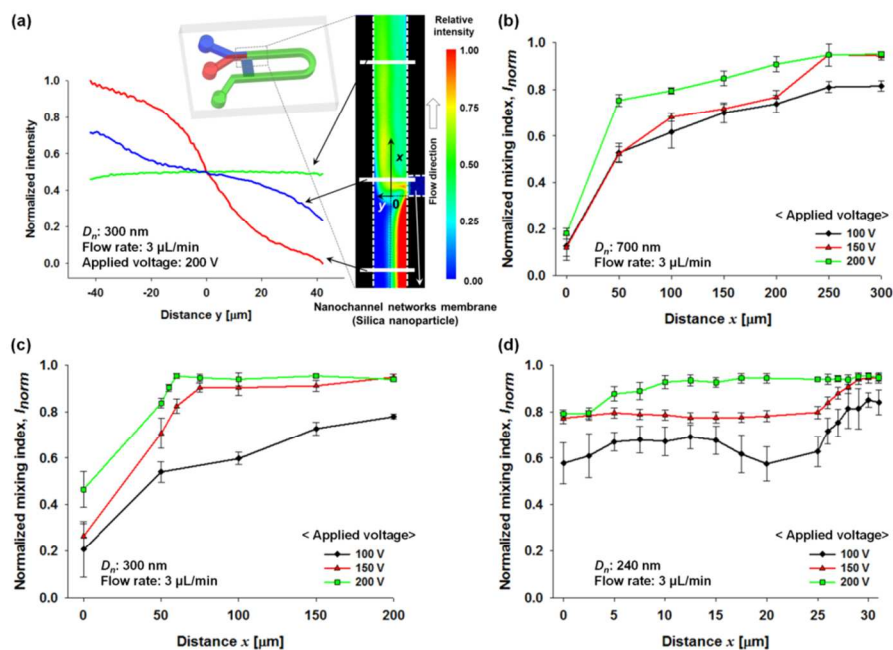


Fig. 2 (a) Fluorescent image and its normalized intensity profiles in y direction from upstream (red line), near NCNM (blue line) and downstream (green line). Normalized mixing index along the fluid flow for variation in voltage and nanoparticle diameters (D_n) of (b) 700 nm. (c) 300 nm. (d) 240 nm.

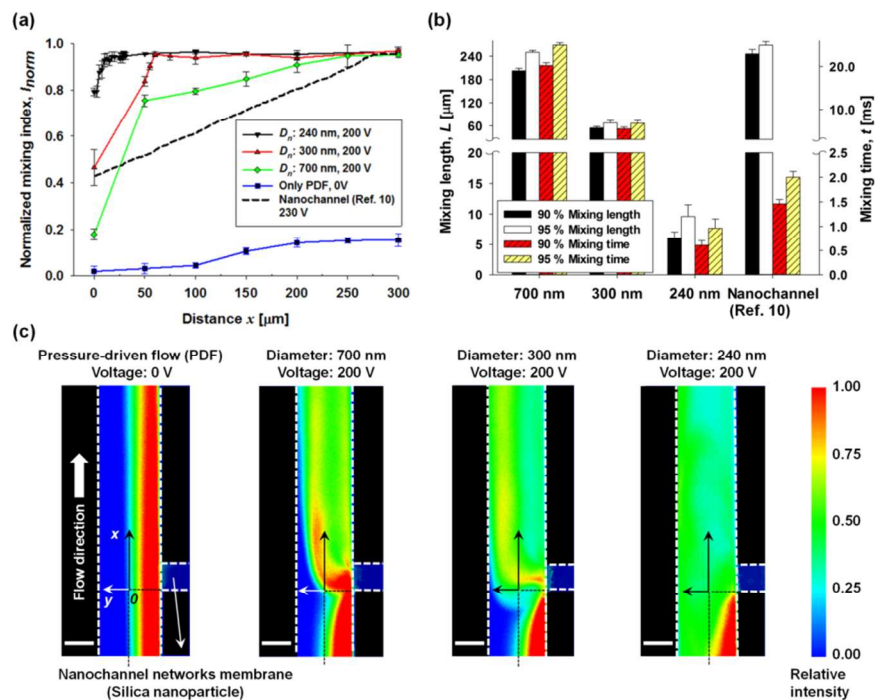


Fig. 3 (a) Normalized mixing index along the fluid flow for variation in nanoparticle diameters. Dash line indicates the normalized mixing index from Lee *et al.*¹⁰ (b) Bar plots for mixing time (t , right axis) and mixing length (L , left axis) at $I_{norm} = [5\%, 95\%]$ and $[10\%, 90\%]$. Bar plot for conventional nanochannel is from Lee *et al.*¹⁰ (c) Fluorescent images for variation in nanoparticle diameters (scale bars: $50 \mu\text{m}$).

Fig. 3(a) shows the total merged mixing index profiles for applied voltage of 200 V. It indicates that the mixing completion seems established further upstream as D_n is reduced from 700 nm to 240 nm. From these experimental data, we calculated the mixing completion length, L (x value where the mixing is completed) and the mixing completion time, t , to characterize the trends. We first

defined two each of L and t , one between $I_{norm} = 0.05$ and $I_{norm} = 0.95$ and the other between $I_{norm} = 0.10$ and $I_{norm} = 0.90$ to take the uncertainty of the data into account, *e.g.*, some error and some fluctuations.¹⁰ We then calculated a mixing length of $I_{norm} = [5\%, 95\%]$ or $[10\%, 90\%]$ for all the curves and divided this mixing length by a flow velocity to obtain a mixing time. The flow velocity

could be obtained from the pre-set flow rate and the cross-sectional area of deep channel (height \times width = 50 μm \times 100 μm). As shown in **Fig. 3(b)**, the complete mixing length and the time are reduced as D_n decrease. Here, the black and the empty bar plots indicates the L , the red and the yellow bar plots indicates the t for $I_{norm} = [5\%, 95\%]$ and $[10\%, 90\%]$, respectively. The counter-ion concentration in the nanopores increases with the decrease of the D_n and it results in the higher conductivity. Irrespective of the diameter of the nanoparticles, the close-packed nanoparticle with FCC structure has the same packing efficiency (volume of space occupied by the spheres/total volume) and its value is 74.05 % in this case. Therefore, if the nanoparticles are ideally self-assembled within the same volume of the shallow channel, the smaller D_n has larger surface area, which increases the electrical conductance of NCNM. This higher conductance induces the stronger propagation of the ion concentration polarization (ICP). The ability of the propagation of the ICP can be well defined by the ratio of bulk to surface conductance, $c_{0,r}^*h_n^*$, which is the inverse form of Dukhin number.¹⁷⁻¹⁹ When $c_{0,r}^*h_n^*$ is lower than the unity, *i.e.*, $c_{0,r}^*h_n^* = (\mu_+z_+ - \mu_-z_-)Fh_n c_{0,r} / (-2\mu_+\sigma) \ll 1$, the ion depletion boundary from ICP will propagate as shock wave. Moreover, the lower $c_{0,r}^*h_n^*$ induces the stronger electric field gradients at the depletion region. Here, $c_{0,r}$ is the background electrolyte concentration in reservoir (0.1 mM KCl); h_n is the diameter of the nanopore (when D_n is 240 nm, 300 nm, and 700 nm, h_n is 36, 45, and 105 nm, respectively); μ_+ and μ_- are the motilities of the positive and negative ions ($\mu_{K^+} \approx 7.62 \times 10^{-8}$ m²/V/s, $\mu_{Cl^-} \approx 7.19 \times 10^{-8}$ m²/V/s),^{20, 21} z_+ and z_- are the valence of the positive and negative ions ($z_+, z_- = 1, -1$); F is the Faraday constant (96485 C \cdot mol⁻¹); σ is the surface charge density of nanochannel. We used the average value of surface charge density with -0.0215 C/m² from reference values (-0.018 C/m² and -0.025 C/m²).^{22, 23} At D_n with 700 nm, 300 nm, and 240 nm, $c_{0,r}^*h_n^*$ is about 0.047, 0.020, and 0.016, respectively. These results mean that the lower D_n induces the stronger electric field gradients at the depletion shock boundary and it creates the larger vortices near NCNM. The fluorescent image in **Fig. 3(c)** shows that as the D_n becomes smaller, the larger vortex structure is established near NCNM at the same applied voltage and it brings the start of the mixing for further upstream from NCNM (*i.e.* $x < 0$).

In this paper, we achieved the best performance at D_n of 240 nm. There values are $L = 6.10 \pm 0.96$ μm and $t = 0.61 \pm 0.10$ ms for $I_{norm} = [10\%, 90\%]$ and $L = 9.62 \pm 1.89$ μm and $t = 0.96 \pm 0.19$ ms for $I_{norm} = [5\%, 95\%]$. The fixed conditions are the applied voltage of 200 V, 0.1 mM KCl concentration, and the flow rate of 3 $\mu\text{L}/\text{min}$. Comparing these mixing performance in direct with the conventional straight nanochannel,¹⁰ we obtained about 2-fold shorter mixing time and 34-folds shorter mixing length in average of $I_{norm} = [5\%, 95\%]$ and $[10\%, 90\%]$: As shown in **Fig. 3(a) and (b)**, Lee *et al.* achieved $L = 246 \pm 11.31$ μm and $t = 1.46 \pm 0.09$ ms for $I_{norm} = [10\%, 90\%]$ and $L = 268 \pm 9.19$ μm and $t = 2.00 \pm 0.12$ ms for $I_{norm} = [5\%, 95\%]$. The fixed conditions were the applied voltage of 230 V, 0.1 mM KCl concentration, and the flow rate of 10 $\mu\text{L}/\text{min}$. The reason of the better achievement of mixing performance in our proposed system is the increase of the effective interfacial area from 3D nanochannel networks from the assembled nanoparticles. Lee *et al.* obtained best value when they used 100 units of 10 μm wide nanochannels (height of 55.3 nm) and its effective interfacial area was about 55 μm^2 . Moreover, the

total length of nanochannel array (width of nanochannel + gap between nanochannels) was 1990 μm . In our case, the cross-section area of shallow channel is $h_s \times w_s = 25$ $\mu\text{m} \times 50$ μm and effective interfacial area (here, 21.5 % of the cross-section area of shallow channel, *i.e.*, $0.215h_s w_s$, see more details in **Sec. III, ESI†**) is about 269 μm^2 . The low flow rate (3 $\mu\text{L}/\text{min}$) and high voltage (200 V) in the mixing performance however would limit the application of our device. It can in principle be resolved by increasing the height of the shallow channel or using the different kind of material of nanoparticles, *e.g.*, polystyrene. Choi *et al.* recently have shown that the higher shallow channel promotes the ion flux in NCNM and also the hydrophobicity of polystyrene surface property can amplify the hydrodynamic slippage result in increase of the conductance of NCNM.⁶ We believe therefore these easily control of NCNM electrical properties can achieve the enhanced mixing performances.

Conclusions

In this article, we proposed an active micromixer having 3D nanochannel networks constructed by the spatially controlled nanoparticle assembly in a cost effective and simple fashion. It induced vortex generation due to non-equilibrium electrokinetics near NCNM that allowed the large effective interfacial area. The mixing performance in the proposed system was investigated according to variation of the diameter of the nanoparticles, and we found that the high surface conductance that occurred in small sized nanoparticles could attain the shorter mixing time and the mixing length. We believe that much higher mixing performance such as shorter mixing time, shorter mixing length, higher flow rate, and lower voltage will be accomplished easily by selecting the proper size of nanoparticles, geometrically controlling the shallow channel, and using different kinds of nanoparticle materials.

Acknowledgements

This work was supported by Basic Science Research Program (2013R1A1A2073271), and by National Nuclear R&D Program (2012M2A8A4055325) through the National Research Foundation of Korea funded by Ministry of Science ICT & Future Planning.

Notes and references

Department of Mechanical Engineering, Sogang University, 35 Baekbeom-ro, Mapo-gu, Seoul, 121-742, Korea,

* Correspondence should be addressed to Prof. Jungyul Park and Prof. Daejoong Kim: E-mail: sortpark@sogang.ac.kr, daejoong@sogang.ac.kr

† Fabrication process for PDMS microfluidic channels with multilayered design, *In situ* formation of nanochannel networks using nanoparticles, Effective cross sectional area of ideally close-packed homogeneous nanoparticles into the FCC structure, and movie for mixing near NCNM. See DOI: 10.1039/b000000x/

1. E. Choi, H. K. Chang, C. Y. Lim, T. Kim and J. Park, *Lab Chip*, 2012, 12, 3968-3975.
2. J. S. Shim and C. H. Ahn, *Lab Chip*, 2012, 12, 863-866.
3. E. Choi, K. Kwon, D. Kim and J. Park, *Lab Chip*, 2015, 15, 168-178.
4. Y. Zeng and D. J. Harrison, *Anal. Chem.*, 2007, 79, 2289-2295.
5. Y. Lei, F. Xie, W. Wang, W. Wu and Z. Li, *Lab Chip*, 2010, 10, 2338-2340.

Lab on a chip

6. E. Choi, K. Kwon, D. Kim and J. Park, *Lab Chip*, 2015, 15, 512-523.
7. E. Choi, K. Kwon, S. J. Lee, D. Kim and J. Park, presented in part at the Proc. of Micro Electro Mechanical Systems (MEMS), 2012 IEEE 25th International Conference, Paris, Jan. 29-Feb. 2, 2012.
8. A. Syed, L. Mangano, P. Mao, J. Han and Y. A. Song, *Lab Chip*, 2014, 14, 4455-4460.
9. I. Cho, G. Y. Sung and S. J. Kim, *Nanoscale*, 2014, 6, 4620-4626.
10. S. J. Lee and D. Kim, *Microfluid. Nanofluid.*, 2012, 12, 897-906.
11. S. H. Ko, Y. A. Song, S. J. Kim, M. Kim, J. Han and K. H. Kang, *Lab Chip*, 2012, 12, 4472-4482.
12. S. J. Kim, S. H. Ko, K. H. Kang and J. Han, *Nat. Nanotechnol.*, 2013, 8, 609-609.
13. D. Kim, A. Raj, L. Zhu, R. I. Masel and M. A. Shannon, *Lab Chip*, 2008, 8, 625-628.
14. Q. S. Pu, J. S. Yun, H. Temkin and S. R. Liu, *Nano Lett.*, 2004, 4, 1099-1103.
15. S. J. Kim, Y. C. Wang, J. H. Lee, H. Jang and J. Han, *Phys. Rev. Lett.*, 2007, 99, 044501.
16. G. Yossifon and H. C. Chang, *Phys. Rev. Lett.*, 2008, 101, 254501.
17. T. A. Zangle, A. Mani and J. G. Santiago, *Chem. Soc. Rev.*, 2010, 39, 1014-1035.
18. T. A. Zangle, A. Mani and J. G. Santiago, *Langmuir*, 2009, 25, 3909-3916.
19. A. Mani, T. A. Zangle and J. G. Santiago, *Langmuir*, 2009, 25, 3898-3908.
20. T. Okada, H. Satou, M. Okuno and M. Yuasa, *J. Phys. Chem. B*, 2002, 106, 1267-1273.
21. S. Koneshan, J. C. Rasaiah, R. M. Lynden-Bell and S. H. Lee, *J. Phys. Chem. B*, 1998, 102, 4193-4204.
22. Z. Chen, Y. S. Wang, W. Wang and Z. H. Li, *Appl. Phys. Lett.*, 2009, 95, 102105.
23. R. B. Schoch and P. Renaud, *Appl. Phys. Lett.*, 2005, 86, 253111.